EAGE

CONFERENCE & EXHIBITION
NEAR SURFACE GEOSCIENCE'21

Imaging hydrogeological and mechanical parameters in landslides through geophysical data fusion: the Hofermühle site

Nathalie Roser[1] , Matthias Steiner[1], Margherita Stumvoll[2], Timea Katona[1], Thomas Glade[2], Adrián Flores Orozco[1]

[1] Research Unit Geophysics, Department for Geodesy and Geoinformation, TU Wien, Wiedner Hauptstraße 8, 1040 Vienna
[2] Department of Geography and Regional Research, University of Vienna, Universitaetsstraße 7, 1010 Vienna

Summary

We applied a data-fusion strategy based on imaging results obtained from joint inversion of seismic and electric data sets, independent inversion of induced polarization data and multichannel analysis of surface waves to solve for mechanical and petrophysical parameters in a shallow landslide in Austria. Seismic data was used to estimate the Poisson's ratio and a subsurface density model was defined by rock, water and air contents retrieved from the joint inversion. Based on these subsurface models the elastic moduli shear and Young's moduli were derived to characterize the subsurface in terms of material stiffness. Ground truth data was used to evaluate the resolved models and showed good agreement to the imaging results. The combination of all data sets provided an imaging framework allowing to distinguish lithological units and revealing spatial information on the saturation state and stiffness of the subsurface to accurately define the characteristics of a shallow landslide.

Imaging hydrogeological and mechanical parameters in landslides through geophysical data fusion: the Hofermühle site

Introduction

Landslide investigations are challenging as they involve the quantification of both mechanical and hydrological parameters. Such parameters can be directly retrieved by intrusive methods, such as dynamic probing or percussion drilling. However, these measurements are spatially constrained and their resolution may be limited in complex conditions with high variability as those found in landslide areas (Flores Orozco et al., 2018). To improve the spatial resolution, geophysical methods are frequently applied as they permit quasi-continuous investigations of subsurface properties to delineate the geometry of the sliding plane or determine the spatial distribution of the hydrogeological and mechanical parameters (e.g. Samyn et al., 2012; Revil et al., 2020). On the one hand, seismic methods provide information about changes in the elastic properties, linked to mechanical properties that permit the discrimination between the sliding material and the bedrock (Uhlemann et al., 2016c). On the other hand, electrical methods provide information about changes in the electrical resistivity related to changes in water and clay content (e.g. Flores Orozco et al., 2018; Gallistl et al., 2018), which in turn control groundwater flow and can predict the increase in pore-pressure and the triggering of slides.

In this study, we present the combined application of seismic and electrical methods to gain a better understanding of a shallow landslide in Austria. In particular, we applied the multichannel analysis of surface waves (MASW), seismic refraction tomography (SRT), as well as induced polarization in frequency (FDIP) and time domain (TDIP). Independent inversion of the data sets reveals good agreement between the geophysical models and direct investigations at the site, as presented in Figure 1. However, such analysis does not quantify variations in the hydrogeological and mechanical parameters of interest. To overcome this, we conducted a joint inversion of the seismic travel times obtained from SRT and apparent electrical resistivities from IP data sets to solve for petrophysical parameters (rock, water, and air content) and combine these with MASW results to derive elastic parameters, i.e., the shear and Young's moduli, in an imaging framework.

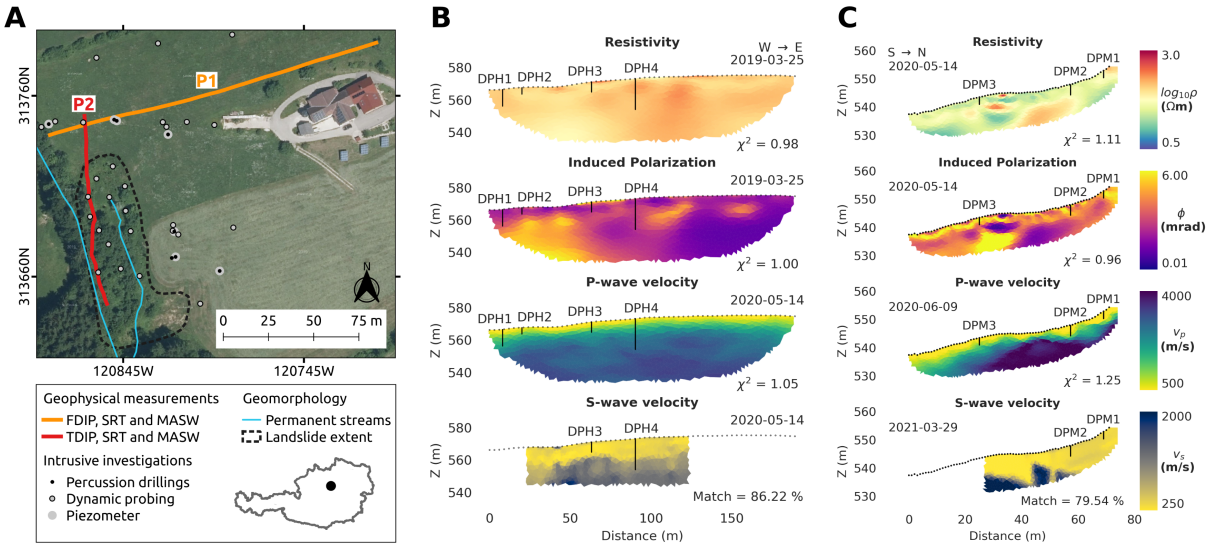

Figure 1 *(**A**) Overview of the field site, geophysical survey locations and existing geotechnical measurements. Electrical resistivity, induced polarization, and seismic P- and S-wave velocity tomograms obtained from individual inversion of measurements along profile P1 oriented roughly W-E (**B**) and profile P2 oriented S-N (**C**). Individual data fit (χ^2 or Match), measurement orientation and date of the measurements are shown next to the tomograms. Black dots indicate sensor positions, black lines indicate the location and maximum depth reached with ramming soundings (DPH or DPM).*

Investigation of the "Hofermühle" landslide

The Hofermühle landslide, located in a hydrological catchment area near Waidhofen a. d. Ybbs (Lower Austria), is characterized by the complex geological transition zone between Flysch and Klippenzone (Schnabel, 1980). The geophysical measurements were conducted along two profiles P1 and P2 illustrated in Figure 1a. Line P1 (orientated roughly W-E) is located above the main active landslide area crossing two subsidence areas. Line P2 (oriented S-N) is located within the active landslide area and extends across the landslide border at the top of the slide. Direct information obtained through dynamic probing heavy (DPH) and medium (DPM) were used to evaluate the geophysical results. We collected seismic data with the DMT Summit data acquisition system and used a 7.5 kg sledgehammer to generate seismic waves. 48 vertical geophones with a corner frequency of 30 Hz deployed with 2 m spacing were used for the SRT survey with shot positions located between the geophones. Four shots were stacked at each shot position to improve the signal-to-noise ratio. For the surface wave measurements, we used a land streamer with 24 vertical geophones (corner frequency 4.5 Hz). We moved the land streamer consecutively along the profile and acquired a dispersion curve for a forward and reverse offset shot. Additional dispersion curves, based on inline shots registered by the first and last 12 geophones respectively, increase the spatial resolution of the MASW investigations. For the electrical measurements, apparent resistivity (ρ_a) and phase (ϕ_a) data were collected in the frequency domain in line P1 (using a DAS-1) and in time domain in line P2 (using a Syscal SwitchPro72). FDIP data were collected at 1 Hz, TDIP data with a pulse length of 500 ms or 1 s, respectively. All measurements were conducted using a Dipole-Dipole (DD) skip-0 (dipole length given by the electrode spacing) configuration with all possible levels. Reciprocal readings were collected on line P2 to quantify the data error. Survey geometries and measurement settings are summarized in Table 1.

Table 1 *Measurement set-up*

	Electrical measurements					Seismic measurements		
	Electrode interval	Electrode number	Array	Domain	Frequency or pulse length	Geophone interval	Geophone number	Corner frequency
P1	3 m	64	DD	FDIP	1 Hz	2 m	48/74	30/4.5 Hz
P2	1/1.5 m	72	DD	TDIP	1/0.5 s	2 m	48/72	30/4.5 Hz

Elastic moduli derived through combination of petrophysical joint inversion and MASW

The SRT and IP data sets were independently inverted (see Figure 1bc) using the open-source library pyGIMLi (Rücker et al., 2017). Moreover, SRT and DC resistivity data were jointly inverted through a modified version of the petrophysical joint inversion (PJI) scheme developed by Wagner et al. (2019) from well-established petrophysical relations between seismic P-wave velocities (v_p) and electrical resistivities (ρ). The modified PJI scheme considers the soil to be composed of volumetric fractions of rock (f_r), water (f_w) and air (f_a) described by a volume conservation constraint as:

$$f_r + f_w + f_a = 1 \tag{1}$$

We use the results obtained through the PJI to derive a bulk density D_bulk model satisfying:

$$D_{bulk} = D_r \cdot f_r + D_w \cdot f_w + D_a \cdot f_a \tag{2}$$

where D_r denotes the density of the solid rock matrix, D_w the density of water, D_a the density of air. The input parameters used for the application of the PJI on line P1 are presented in Table 2, where λ denotes the smoothness regularization parameter, *zWeight* the ratio between vertical to horizontal smoothing, and err_{tt} and err_{ρ_a} the data errors estimated for the SRT and DC resistivity data, respectively. Adequate values for the regularization and Archie parameters a, m, n were determined by methodical variation of a wide range of values for each parameter. The error-weighted data fit χ^2 was found to be 1.14 indicating that the resolved models explain the observed data (Günther et al., 2006).

Table 2 *Model parameters for the application of the PJI on profile P1.*

Regularisation		Data error		Archie parameters			Material properties			
λ	$zWeight$	err_{tt}	$err\rho_a$	a	m	n	v_r	v_w	v_a	ρ_w
107	0.1	1.5 ms	7 %,	1.8	1.5	2	3500 m/s	1500 m/s	330 m/s	1 Ωm

The surface wave data are used to solve for a shear wave velocity (v_s) model by taking advantage of the dispersion in Rayleigh-type surface waves. For the MASW, we use the commercial software ParkSEIS (Park et al., 1999). We describe the elastic properties of the subsurface materials with the shear (μ) and Young's modulus (E), both providing a measure for the material stiffness. We calculate these elastic moduli based on the obtained subsurface models for D_{bulk} , v_s and v_p as:

$$\mu = D_{bulk} \cdot v_s^2 \tag{3}$$

$$E = 2 \cdot D_{bulk} \cdot v_s^2 \cdot (1 + \sigma) \tag{4}$$

where σ denotes the Poisson's ratio, which is related to the saturation extend of soils (Uhlemann et al., 2016c). σ can be calculated from v_p and v_s as:

$$\sigma = \frac{(v_p^2 - 2 \cdot v_s^2)}{2 \cdot (v_p^2 - v_s^2)} \tag{5}$$

Results

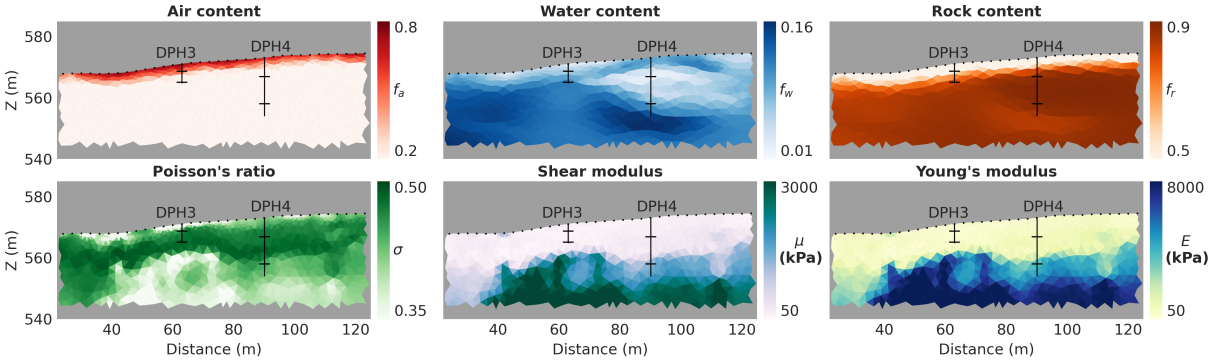

Figure 2 *Petrophysical and mechanical parameters resolved for measurements along profile P1. The imaging results are clipped to the extent of the surface wave survey. Vertical black lines indicate the location and maximum depth reached with DPH soundings. Horizontal black lines mark some sharp transitions in material strength (DPH blow counts > 15)). In DPH3 blow counts of 34 and 23 and in DPH4 blow counts of 28 and 41 are indicated by the upper and lower lines, respectively.*

DPH and DPM conducted along P1 (illustrated in Figure 2) reveal generally low soil strengths (blow count < 4) in near-surface areas (depths < 3 m). DPH3 is characterized by two strongly compacted layers. The first, thin layer is observed at 2.3-2.4 m depth, followed by low to medium soil strengths (blow counts between 1-8). Considering the low seismic velocities observed in the same depth, the sudden increase in blow counts likely indicates a contact between loose sediments on top of denser but still loose material. Similar conclusions are drawn for the second sharp transition in DPH3 at 5.9 m depth and in DPH4 at 6.2 m depth. Additionally, DPH4 shows a clear change in soil strength at 15.1 m depth, corresponding to the strong contrast in seismic velocities observable in the seismic models. This sharp transition most likely separates the firm bedrock below 15 m depth from weathered material on top. Petrophysical and mechanical parameters resolved through the data fusion strategy are generally consistent with the dynamic probing data suggesting that the resolved models are plausible. The shallow subsurface (< 5 m) is characterized by high air content and low saturation and rock content; while deeper

units show a higher water and rock content, as expected for more consolidated materials. We observe high saturation in the West corresponding to higher values of Poisson's ratio ($\sigma > 0.4$), likely indicating an area with increased clay content, which is in agreement with higher IP phase values found in the vicinity. Between approximately 2 to 15 m depth the subsurface is characterized by high values of σ (> 0.4), corresponding to high IP phase values and saturation, which is in contrast with the unit below. This is consistent with the changes in soil strength observed in DPH4 at 15.1 m depth. We therefore assume that values above 0.4 indicate saturated clays or sand, while lower values most likely correspond to partially saturated silt and sand (Uhlemann et al., 2016c). Shear and Young's moduli show generally spatially consistent features and thus indicate soft materials in the upper layer (lower values of μ and E) and firm materials in the second layer.
IP and σ images as well as laboratory analysis of sediments collected after drilling suggest a considerable amount of clay at the site. However, surface conduction is not taken into account in the used petrophysical model, thus, misleading possible results. Ongoing work considers the inclusion of surface conductivity in the PJI, as proposed in the talk by Steiner et al. (2021).

Conclusions

In our study, we present a data fusion strategy based on imaging results obtained through the PJI of SRT and ERT data, independent inversion of IP data, and MASW. We successfully applied this strategy for data collected at the Hofermühle landslide to characterize the subsurface in terms of mechanical and petrophysical properties. Our results demonstrate a good agreement between the resolved models and the ground truth information available from direct investigations conducted at the site. This leads to the assumption that the application of our strategy on the measurements in the active landslide area has the potential to spatially characterize slope characteristics.

References

Flores Orozco, A., Gallistl, J., Bücker, M., Steiner, M. and Williams, K.H. [2018] Complex-conductivity imaging for the understanding of landslide architecture, *Engineering Geology*, **243**, 241-252.

Gallistl, J., Weigand, M., Stumvoll, M., Ottowitz, D., Glade, T. and Flores Orozco, A. [2018] Delineation of subsurface variability in clay-rich landslides through spectral induced polarization imaging and electromagnetic methods, *Engineering Geology*, **245**, 292-308.

Günther, T., Rücker, C. and Spitzer, K. [2006] Three-dimensional modelling and inversion of dc resistivity data incorporating topography—II. Inversion. *Geophysical Journal International*, **166**(2), 506–517.

Park, C.B., Miller, R.D. and Xia, J. [1999] Multi-channel analysis of surface waves (MASW). *Geophysics*, **64**(3), 800-808.

Revil, A., Ahmed, A.S., Coperey, A., Ravanel, L., Sharma, R. and Panwar, N. [2020] Induced polarization as a tool to characterize shallow landslides. *Journal of Hydrology*, **589**, 125369.

Rücker, C., Günther, T. and Wagner, F. [2017] pyGIMLi: An open-source library for modelling and inversion in geophysics. *Computers & Geosciences*, **109**, 106-123.

Samyn, K., Travelletti, J., Bitri, A., Grandjean, G. and Malet, J.-P. [2012] Characterization of a landslide geometry using 3D seismic refraction traveltime tomography: The La Valette landslide case history. *Journal of Applied Geophysics*, **86**, 120-132.

Schnabel, W. [1980] Die Geologie des Voralpengebietes im Abschnitt Waidhofen an der Ybbs - Ybbsitz - Gresten. *Waidhofner Heimatblätter*, 13-27.

Steiner, M. [2021] Resolving hydrogeological parameters through joint inversion of seismic and electric data considering surface conductivity. **Submitted to** *82th EAGE Conference & Exhibition*, Extendend Abstract.

Uhlemann, S., Hagedorn, S., Dashwood, B., Maurer, H., Gunn, D., Dijkstra, T. and Chambers, J. [2016c] Landslide characterization using P- and S-wave seismic refraction tomography—The importance of elastic moduli. *Journal of Applied Geophysics*, **134**, 64–76.

Wagner, F., Mollaret, C., Günther, T., Kemna, A. and Hauck, C. [2019] Quantitative imaging of water, ice and air in permafrost systems through petrophysical joint inversion of seismic refraction and electrical resistivity data. *Geophysical Journal International*, **219**(3), 1866–1875.